



Regular article

In silico analysis of synthetic multispecies biofilms for cellobiose-to-isobutanol conversion reveals design principles for stable and productive communities

Ayushi Patel ^a, Ross P. Carlson ^b, Michael A. Henson ^{a,*}^a Department of Chemical Engineering and the Institute for Applied Life Sciences, University of Massachusetts, Amherst, MA 01003, USA^b Department of Chemical and Biological Engineering, Montana State University, Bozeman, MT 59717, USA

ARTICLE INFO

ABSTRACT

Keywords:

Metabolic modeling
 Multispecies biofilms
 Renewable biochemicals
 Isobutanol production

Efficient, large-scale conversion of plant-derived feedstocks to commodity chemicals remains a substantial technological challenge with enormous potential for societal benefits. Most research efforts have focused on metabolic engineering of model organisms for planktonic cell cultures in well-mixed suspension bioreactors. We utilized *in silico* metabolic modeling to explore the potential benefits of an alternative design strategy based on combining bacterial strains with complementary metabolic functions within high density, multispecies biofilms. We simulated four alternative system designs, each of which consisted of an anaerobic cellulolytic bacterium which degraded cellobiose to glucose, an aerobic *Escherichia coli* strain engineered for glucose-to-isobutanol conversion, and an aerobic or anaerobic byproduct consumer for metabolizing growth-inhibiting organic acids such as acetate secreted by the other two strains. Our simulations predicted dramatically different cellobiose-to-isobutanol conversion capabilities depending on the metabolic compatibility of the three bacteria. Important design considerations included glucose competition between the cellulolytic and isobutanol-producing bacteria, O₂ competition between the isobutanol-producing and byproduct-consuming bacteria, organic acid matching between the cellulolytic and byproduct-consuming bacteria and the degree of metabolic redundancy between the community members. We believe that these design principles will be widely applicable to synthetic biofilm communities engineered to perform other bioconversion tasks.

1. Introduction

Biocatalysts such as bacteria, yeasts and fungi have broad potential for sustainable bioprocessing applications [1–4]. Traditionally, model microbial strains have been engineered for biosynthesis of medically and industrially relevant compounds [5–7]. A particularly notable success is the large-scale, industrial development of an *Escherichia coli* strain engineered for conversion of glucose to the polymer precursor 1,3-propanediol [8,9]. However, the single microbe strategy has proven to have serious limitations including the difficulty of incorporating multiple non-native functions [9,10], reduced growth due to metabolic burden induced by pathway engineering [9,11] and increased cellular stress due to secretion of inhibitory byproducts [3,10]. These pitfalls can be circumvented by designing synthetic microbial communities which take advantage of the unique metabolic capabilities of well-characterized species to collectively achieve a desired conversion

task [12,13]. A prerequisite for a functional community is stable, coexistence of the individual strains, which can be highly challenging in well-mixed planktonic bioreactors due to the different physiological requirements of each microbe (e.g. aerobic vs. anaerobic metabolism).

Most bacteria naturally grow as multispecies biofilms due to their ability for surface attachment and the inherent advantages of close proximity for metabolite exchange [14,15]. Synthetic multispecies biofilms provide an effective means to promote community stability [16] while simultaneously achieving high cell densities needed for large-scale biochemical production [1,17]. Spatial gradients allow strains with different physiologies to coexist due to the creation of diffusion-controlled metabolic niches within the biofilm [1,18]. By strategically supplying electron donors and acceptors at different biofilm interfaces, nutrient and byproduct gradients can be tuned to establish spatial distributions to promote synergistic strain interactions [15,16]. Biofilm reactors provide a scalable technology for exploiting

* Corresponding author.

E-mail address: mhenson@umass.edu (M.A. Henson).

the high cell densities and volumetric productivities achievable with the biofilm mode of growth [1,19,20]. Other advantages of biofilm reactors compared to planktonic suspension cultures include minimal mixing requirements, reduced water requirements and improved robustness to cellular stresses due to spatial organization [1,14,17].

Natural and synthetic biofilm communities have been applied to diverse engineering problems including sewage treatment [21], industrial wastewater treatment [22–24], microbial fuel cells [25–27] and metal extraction from low grade ores [28]. A particularly important and largely unsolved problem is large-scale biochemical production from renewable lignocellulosic biomass [20,29,30] to reduce reliance on petrochemical technologies [31,32]. Lignocellulosic biomass generated from crop, agricultural and forest residues is a complex combination of biopolymers including cellulose, hemicelluloses, pectin and lignin [20, 31]. Sugars derived from enzymatic deconstruction of lignocellulose have significant potential for large-scale biochemical synthesis [20,33, 34]. Studies have demonstrated the potential of monoculture biofilms for conversion of plant-derived feedstocks to renewable biochemicals [19,35–39]. The development of synthetic microbial communities for biochemical production has recently garnered considerable interest [3, 5,12,32]. Representative studies based on planktonic suspension cultures include cellulose-to-ethanol conversion with a coculture of the cellulolytic bacterium *Clostridium phytofermentans* paired with the yeast *Saccharomyces cerevisiae* [34] and cellulose-to-isobutanol conversion with the cellulolytic fungus *Trichoderma reesei* and a *E. coli* strain metabolically engineered for isobutanol synthesis [32]. Synthetic biofilm communities have received less attention, although one notable study successfully cultured *T. reesei*, *S. cerevisiae* and the pentose-fermenting yeast *Scheffersomyces stipitis* in a membrane biofilm reactor for conversion of dilute acid pretreated wheat straw to ethanol [20].

A key bottleneck to the development of productive and robust synthetic communities is the difficulty in identifying compatible microbial strains and favorable culture conditions. The lack of established design principles substantially impedes the innovation process and tends to render each community design as a one-off effort lacking extensibility to other bioconversion systems. Numerous studies have demonstrated that metabolic modeling represents a valuable complementary tool to mixed-culture experiments for limiting the community design space and identifying promising systems for experimental testing [40–44]. To this end, we have developed a biofilm modeling framework that combines genome-scale metabolic reconstructions of individual bacteria, species-specific uptake kinetics for supplied nutrients and crossfed metabolites, and reaction-diffusion equations for extracellular variables to generate spatially-resolved predictions of strain metabolic interactions [45–48]. The modeling approach has been applied to the design of two-strain biofilm communities to demonstrate the value of incorporating a secondary, acetate-consuming bacterium to detoxify the environment and relieve acetate-induced growth inhibition of a primary bacterium [45,49]. The first system consisted of a wild-type *E. coli* strain combined with a mutant *E. coli* strain that was engineered to eliminate glucose metabolism and allow aerobic acetate uptake. The coculture biofilm model was able to qualitatively reproduce experimentally observed behavior of enhanced biomass accumulation compared to a monoculture biofilm of wild-type *E. coli* [15]. The second system was computationally designed to convert glucose to isobutanol, an important platform chemical used as an oxygenated gasoline component [50–52] and as an industrial solvent [53]. Coculture biofilms consisting of an *E. coli* strain engineered for microaerobic isobutanol synthesis [51] and a wild-type *Geobacter metallireducens* strain for anaerobic acetate consumption were predicted to generate higher isobutanol titers than *E. coli* monoculture biofilms.

In this paper, we utilized our multispecies biofilm modeling framework to investigate four system design alternatives for the conversion of cellobiose to isobutanol. Cellobiose, a disaccharide comprised of two glucose monomers, is a primary product resulting from cellulose

degradation by some anaerobic bacteria [33]. These cellulolytic organisms can further cleave cellobiose to two glucose units through secretion of the enzyme β -glucosidase. Consequently, each candidate design consisted of three strains (Fig. 1a): an anaerobic cellulolytic bacterium that extracellularly degrades cellobiose and can consume both cellobiose and glucose; the engineered *E. coli* strain that performs microaerobic glucose-to-isobutanol conversion [51]; and a byproduct-consuming bacterium that consumes growth-inhibiting organic acids via either aerobic or anaerobic metabolism. We showed that the addition of a cellulolytic organism to our previous two-strains designs required careful matching of the three strains with respect to electron donor and acceptor capabilities. In doing so, we generated several general principles for the design of productive and robust biofilm communities that will be translatable to other bioconversion problems.

2. Theory/calculation

2.1. Bacterial strain metabolic models

Each three-strain synthetic community consisted of an anaerobic cellulolytic bacterium for cellobiose degradation to glucose, a mutant *E. coli* strain engineered for microaerobic glucose-to-isobutanol conversion, and an aerobic or anaerobic byproduct consumer for uptake of organic acids such as acetate secreted by and inhibitory to the other two strains (Fig. 1a). Each strain was modeled with available genome-scale, metabolic reconstructions modified as necessary to represent engineered strains. The isobutanol-producing *E. coli* strain (*Ec-ib*), a mutant *E. coli* strain engineered for aerobic acetate consumption (*Ec-ac*) and a wild-type *Geobacter metallireducens* (*Gm*) strain used for anaerobic acetate consumption were modeled as discussed in our previous publication [45]. The *E. coli* strain JCL260 [51,54] was generated from the iAF1260 reconstruction [54] by adding a heterologous pathway for isobutanol synthesis and deleting six genes associated with formation of undesired byproducts. Similarly, the iAF1260 reconstruction was used to model the *E. coli* strain 403G100 [15] engineered for aerobic acetate consumption by deleting four genes involved in glucose transport and conversion. We used the *G. metallireducens* iAF987 reconstruction [55] without modification.

Two commensal bacteria present in the human gut microbiota were incorporated into the synthetic communities to add cellobiose degradation capabilities. We sought strains which could consume both cellobiose and glucose and secrete the organic acid acetate such that the synthetic communities would possess the common ecological features of biopolymer degradation, nutrient competition and inhibitory metabolite secretion. The Virtual Metabolic Human (VMH) database (PMC6323901; www.vmh.life) contained genome-scale metabolic reconstructions of 379 bacterial strains which could degrade cellobiose and five strains which could degrade cellulose. Because we were interested in extending our modeling work to cellulose-degrading communities in the future, the five stains with this capability were screened according to their ability to degrade cellobiose and secrete organic acids. This screening procedure yielded the anaerobes *Ruminococcus channellensis* 18P13 (*Rc*) and *Cellulosilyticum lentoceum* DSM 5427 (*Cl*) as the two cellulolytic strains used in our communities. These two semi-curated reconstructions required specification of ATP maintenance parameters. Because we were unable to find growth rate data for well controlled cell culture experiments with defined media, the ATP maintenance values were specified such that they affected *in silico* growth predicted by FBA with maximum uptakes rates of cellobiose, glucose and essential amino acids (see Table S3). These values ensured that growth would be limited by ATP production throughout our simulated biofilms. Properties of the five metabolic reconstructions used in this study are summarized in Table S1.

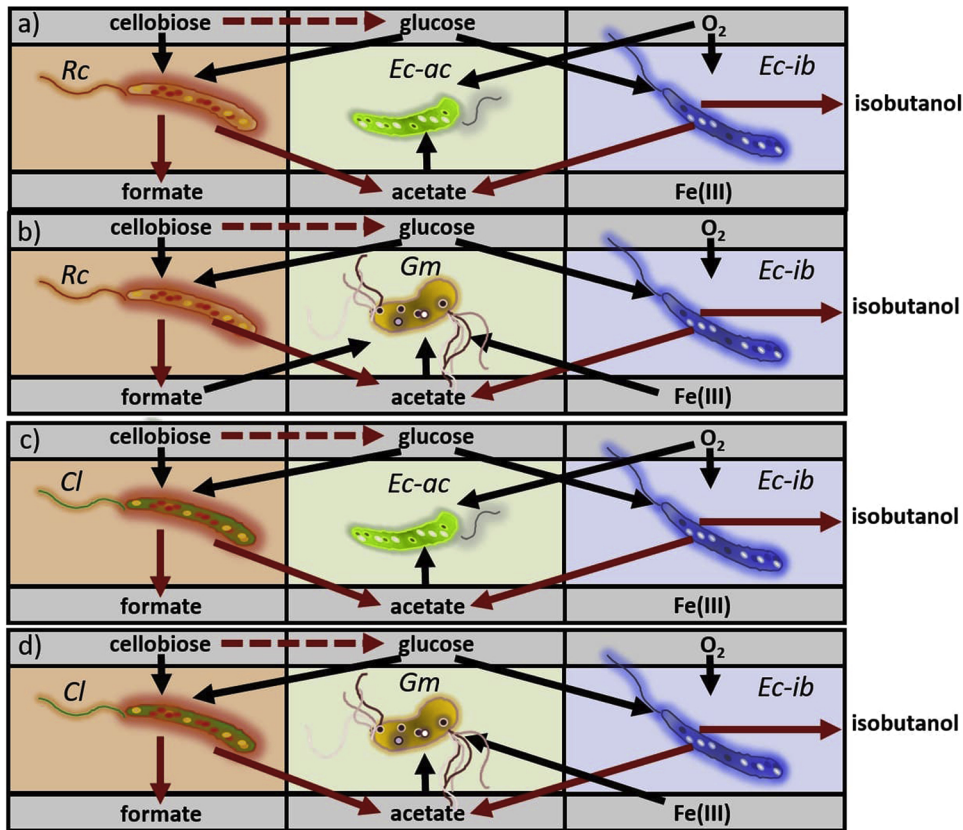


Fig. 1. Conceptual design of three-strain synthetic communities for conversion of cellobiose to isobutanol. (a) Triculture system design 1 consisting of the cellulolytic gut bacterium *Ruminococcus champanellensis* (*Rc*) and a mutant *E. coli* strain engineered for aerobic acetate consumption (*Ec-ac*) paired with isobutanol-synthesizing *E. coli* *Ec-ib*. (b) Triculture system design 2 consisting of the anaerobic organic acid-consuming bacterium *Geobacter metallireducens* (*Gm*) paired with *Rc* and *Ec-ib*. (c) Triculture system design 3 consisting of cellulolytic gut bacterium *Cellulosilyticum lentocellum* (*Cl*) paired with *Ec-ib* paired with *Ec-ac*. (d) Triculture system design 4 consisting of *Cl*, *Ec-ib* and *Gm*.

2.2. Biofilm community designs

We combined the five strains into four synthetic biofilm communities (Fig. 1b–e) to explore the impact of the alternative nutrient competition and byproduct secretion motifs on community stability (*i.e.* coexistence of the three strains) and cellobiose-to-isobutanol conversion efficiency (*i.e.* isobutanol concentration). Flux balance analysis (FBA) showed that the two cellulolytic bacteria differed with respect to their glucose affinity and organic acid secretion patterns (*i.e.* *Rc* was predicted to have higher glucose uptake rates than *Cl* and secreted formate in addition to acetate). The two byproduct consumers differed with respect to the electron acceptors used and organic acids metabolized (*i.e.* *Gm* used Fe (III) and consumed both acetate and formate while *Ec-ac* used O₂ and consumed only acetate).

2.3. Biofilm model formulation

Each synthetic community was modeled *in silico* using our biofilm modeling framework [45–48] that combined genome-scale metabolic reconstructions (GSMs) of the individual strains, nutrient uptake kinetics with inhibition terms for growth-suppressing byproducts, and extracellular mass balances describing diffusion-dominated transport. The biofilm was assumed to have a fixed length *L* with *z* = *L* denoting the surface-biofilm interface where media containing cellobiose, essential amino acids and Fe(III) (for *Gm* containing communities) was supplied through a semi-permeable membrane and *z* = 0 denoting the other end of the biofilm where O₂ was introduced. Spatial gradients were allowed to occur only in the axial direction *z*.

The biomass concentration of strain *i* was described by the reaction-diffusion equation [45],

$$\frac{\partial X_i}{\partial t} = \mu_i X_i + D_i \frac{\partial^2 X_i}{\partial z^2} - k_{di} X_i \quad (1)$$

where *t* denotes time, *X_i(z,t)* is the biomass concentration, μ_i is the cellular growth rate, *D_i* is a diffusion coefficient that accounts for passive cellular movement in the biofilm and *k_{di}* is the cellular death rate. The growth rate was described by the function,

$$\mu_i = \mu_{is} - k_P(\alpha_h + \beta_h) \quad (2)$$

where μ_{is} is the specific growth rate calculated from the GSM, *k_P* is an enzyme penalty constant defined only for the cellulolytic organism, and α_h and β_h are the basal and induced synthesis rates, respectively, of the β -glucosidase enzyme (see below). The enzyme synthesis penalty was added to the GSM-calculated growth rate as a simple means to account for the protein and energy costs associated with enzyme synthesis and secretion which are outside the scope of primary metabolism captured by the reconstruction. The cellular death rate was described by the function,

$$k_{di} = \begin{cases} k_{d0} \text{ for aerobic species} \\ k_{d0} \left(1 + \sqrt{\frac{C_{O_2}}{0.21}} \right) \text{ for anaerobic species} \end{cases} \quad (3)$$

where *k_{d0}* is a constant basal death rate applicable to all strains that accounts for non-specific removal of viable biomass from the biofilm (*e.g.* erosion from biofilm surfaces [56,57], density-driven death encoded through quorum sensing [57] and the additional term accounts for the toxic effects of O₂ on anaerobic species. The biomass equations were solved subject to no-flux boundary conditions imposed at each end of the biofilm,

$$-D_i \frac{\partial X_i(0, t)}{\partial z} = 0, \quad -D_i \frac{\partial X_i(L, t)}{\partial z} = 0, \quad (4)$$

The extracellular concentration of metabolite *k* within the biofilm was modeled as,

$$\frac{\partial C_k}{\partial t} = v_{ik}X_i + D_k \frac{\partial^2 C_k}{\partial z^2} \quad (5)$$

where $C_k(z,t)$ is the metabolite concentration, v_{ik} is the metabolite uptake rate (negative) or secretion rate (positive) calculated from the GSM of cell type i and D_k is the metabolite diffusion coefficient. The metabolite differential equations were solved subject to Robin-type boundary conditions obtained by balancing diffusive and mass transfer fluxes at the two biofilm boundaries,

$$-D_k \frac{\partial C_k(0,t)}{\partial z} = k_{0,k} [C_{b,k}(0,t) - C_k(0,t)], \quad -D_k \frac{\partial C_k(L,t)}{\partial z} = k_{L,k} [C_{b,k}(L,t) - C_k(L,t)] \quad (6)$$

where $C_{b,k}(0)$ and $C_{b,k}(L)$ are bulk concentrations and $k_{0,k}$ and $k_{L,k}$ are corresponding mass transfer coefficients.

Cellobiose was degraded to glucose through the synthesis, secretion and diffusion of β -glucosidase from the cellulolytic bacteria. The extracellular enzyme concentration was described by the transport equation,

$$\frac{dE}{dt} = \alpha_h X + \beta_h X - \gamma_h E + D_E \frac{\partial^2 E}{\partial z^2} \quad (7)$$

where E is the enzyme concentration, α_h is a constant basal synthesis rate, β_h is the induced synthesis rate, γ_h is a constant degradation rate and D_E is the diffusion coefficient. Induced enzyme synthesis was modeled using an expression originally developed for the cellulolytic fungus *T. reesei* [58],

$$\beta_h = \frac{\beta_{hm} C_G}{K_{bh} + C_G} \frac{1}{1 + \frac{C_G}{K_{ibhh}}} \quad (8)$$

where C_G is the glucose concentration, β_{hm} is the maximum rate of induced synthesis, K_{bh} is the saturation constant for induction and K_{ibhh} is the inhibition constant of glucose on induced synthesis. The rate of the reaction cellobiose \rightarrow 2 glucose catalyzed by β -glucosidase was described by the previously developed expression [59,60],

$$v_{dg} = \frac{k_{dg} E C_C}{k_s \left(1 + \frac{C_G}{k_{in}} \right) + C_C} \quad (9)$$

where k_{dg} is the reaction rate constant, C_C is the cellobiose concentration, k_s is the cellobiose saturation constant and k_{in} is the inhibition constant for glucose. The β -glucosidase differential equation was solved subject to Robin-type boundary conditions,

$$-D_E \frac{\partial E(0,t)}{\partial z} = k_{0,E} [E_b(0,t) - E(0,t)], \quad -D_E \frac{\partial E(L,t)}{\partial z} = k_{L,E} [E_b(L,t) - E(L,t)] \quad (10)$$

Nutrient uptake kinetics were modeled by Michaelis-Menten expressions with byproduct inhibition terms [45],

$$v_{ij} = -\frac{v_{ij,max} C_j}{K_{ij+} C_j} \max \left(\prod_{k=1}^m \left(1 - \frac{C_k}{C_{ik,max}} \right), 0 \right) \quad (11)$$

where v_{ij} is the transport-limited uptake of nutrient j by strain i imposed as a lower bound in the associated metabolic reconstruction, $v_{ij,max}$ is the maximum uptake rate, C_j is the concentration of nutrient i , K_{ij} is the saturation constant, C_k is the concentration of byproduct k that inhibits nutrient uptake and $C_{ik,max}$ is the maximum inhibitory concentration of byproduct k at which nutrient uptake will be zero. We considered $m = 3$ inhibitory byproducts, the organic acids acetate and formate and the alcohol ethanol. All four biofilm communities included cellobiose, glucose and O_2 as nutrients. The other nutrients varied for each community depending on the essential amino acids for the cellulolytic bacterium and whether Fe(III) was supplied for *Gm* growth. FBA showed that *Rc* required six amino acids (alanine, cysteine, isoleucine, leucine,

methionine, valine; Table S2) and *Cl* required three amino acids (alanine, cysteine, glutamine). An *in silico* minimal media was developed for each community by combining the nutrient requirements of the three participating bacterial strains.

2.4. Model parameterization and solution

Most model parameters were taken from the literature and our previously published work on two-strain biofilm systems in which model parameters were specified based on qualitative match with coculture biofilm data [15]. We generally assigned the same values across different strains and metabolites for parameters like the biomass diffusion coefficient, biomass mass transfer coefficient and metabolite mass transfer coefficient due to lack of system-specific data in literature. Similarly, strain-independent values were assigned to the basal cellular death rate and the enzyme basal synthesis, degradation and growth penalty constants such that reasonable total biomass concentrations (~ 100 g/L [2]) and enzyme concentrations (~ 1 g/L; [58]). Nutrient uptake parameters for *Ec*-ib, *Ec*-ac [45] and *Gm* [55,61] were taken from previous studies, while *Rc* and *Cl* were assigned glucose and amino acid uptake parameters reported for *E. coli* [47,62] due to lack of species-specific information. A complete set of model parameters for all four communities are listed in Tables S3 and S4.

To mimic a biofilm reactor where consumed nutrients were continuously replenished to attain high productivities required for bioprocess applications, all simulations were performed with constant bulk concentrations of cellobiose (30 mmol/L), total amino acids (4 mmol/L on a C6 basis), O_2 (0.21 mmol/L) and Fe(III) (5 mmol/L if *Gm* was present). Total amino acids were equally split between the essential amino acids on a C6 basis to establish bulk concentrations of each amino acid [63] such that the community designs could be fairly compared. The biofilm thickness was assumed to be constant with a nominal value of 250 microns.

We utilized our previously published biofilm solution strategy based on spatial discretization of the extracellular PDEs followed by integration of the resulting ordinary differential equation (ODE) system with embedded LPs [45–47]. Discretization was performed using central difference approximations with 21 node points to achieve reasonable spatial resolution and numerical accuracy. Discretized biofilm models were solved using the MATLAB code DFBAlab [64], the stiff MATLAB solver ode15s for ODE integration and Gurobi for LP solution. To eliminate the possibility of alternative optima in the intracellular LPs, DFBAlab utilizes lexicographic optimization to ensure a unique set of exchange (uptake and secretion) fluxes. This approach requires the sequential solutions of $n+1$ LPs for each strain, where the first LP is performed for the usual cellular objective of biomass maximization and subsequent LPs are solved to either minimize or maximize a particular exchange flux until all n exchange fluxes are optimized. The lexicographic optimization objectives for all four biofilm community models are listed in Tables S4–S7. We performed dynamic simulations with an initial condition corresponding to a uniform biomass concentration profile of 1 g/L for each strain and consistent metabolite concentration profiles. Dynamic simulations were performed for 1000 h and steady-state concentration profiles at the end of each simulation were captured to demonstrate spatial behavior in the biofilm that was essentially independent of the initial condition. The growth rate of each strain i was plotted in terms of the effective growth rate, defined as $\mu_{e,i} = \mu_i - k_{di}$, to more clearly show the tradeoff between cellular growth and death across the biofilm.

3. Results

3.1. *R. chamarstellensis* and isobutanol-producing *E. coli* system (Coculture design 1)

The four biofilm designs discussed below were assumed to have a fixed thickness of 250 μm with spatial variations occurring only in the axial direction z . The point $z = 250 \mu\text{m}$ represented the surface-biofilm interface and was defined as the bottom of the biofilm. Here the nutrients cellobiose, essential amino acids and Fe(III) (for *Geobacter*-containing communities) were assumed to be supplied through a semi-permeable membrane. The point $z = 0 \mu\text{m}$ represented the top of the biofilm at which point an O_2 saturated liquid phase interface allowed O_2 transfer into the biofilm. Metabolites (nutrients and byproducts) were allowed to exit at both ends of the biofilms, while all mechanisms for biomass elimination (e.g. lysis, attrition, detachment) were modeled through a combination of basal- and nutrient-drive cell death (see Material and Methods).

To demonstrate the advantages of incorporating a third bacterium for scavenging of growth-inhibiting organic acids, we first performed biofilm simulations with the coculture system containing the cellulolytic bacterium *R. chamarstellensis* (*Rc*) and the isobutanol-producing *E. coli* mutant (*Ec*-ib). Spatial concentration profiles showed that O_2 decreased across the biofilm to generate a low O_2 region near the membrane-biofilm interface ($z = 250 \mu\text{m}$), while both cellobiose and glucose were elevated near this interface where cellobiose was supplied, *Rc* preferentially accumulated due to the relatively low O_2 level and the *Rc*-secreted β -glucosidase achieved its maximum concentration (Fig. 2). The six essential amino acids required for *Rc* growth decreased almost linearly from their supply location at the membrane-biofilm interface. While *Ec*-ib utilized the amino acids alanine and valine for growth enhancement near the membrane-biofilm interface (Fig. S1), *Ec*-ib preferentially accumulated near the top of the biofilm ($z = 0 \mu\text{m}$) due to increased O_2 availability. *Rc* competed with *Ec*-ib for glucose and amino

acids and additionally suffered from O_2 inhibition such that *Ec*-ib was predicted to generate much higher biomass concentrations. These biomass concentration profiles were consistent with calculated exchange fluxes (e.g. specific nutrient uptake and byproduct secretion rates), which predicted no *Rc* growth in the upper half of the biofilm. Due to rapid diffusion compared to synthesis, the metabolites secreted by *Rc* (acetate, formate) and *Ec*-ib (acetate, ethanol, isobutanol) were predicted to have flat concentration profiles.

The acetate concentration of 48 mmol/L approached the maximum inhibitory value of 80 mmol/L, reducing *Rc* and *Ec*-ib nutrient consumption and growth through the modeled uptake kinetics (Eq. 11). To quantify the degree of growth suppression caused by each byproduct (acetate, ethanol, formate), we performed additional coculture simulations removing each inhibitory effect by replacing the corresponding byproduct inhibition constant with 10^6 mmol/L to effectively eliminate the effect. The removal of either formate or ethanol inhibition was predicted to have very little impact on biomass and isobutanol concentrations due to relatively low concentrations of these byproducts compared to their inhibitory values (Table 1). By contrast, the removal of acetate inhibition increased the average *Rc* biomass concentration 1450 %, resulting in a 36 % increase in the isobutanol concentration. These predictions suggested that the incorporation of a third strain specializing in acetate consumption could substantially improve system performance.

3.2. *R. chamarstellensis*, isobutanol-producing *E. coli* and acetate-consuming *E. coli* system (Triculture design 1)

We first added the aerobic, acetate-consuming *E. coli* mutant (*Ec*-ac) to the *Rc*/*Ec*-ib coculture system to investigate if the theoretical advantages of eliminating acetate inhibition could be realized in a triculture system (Fig. 1b). Unexpectedly, the isobutanol production performance of the triculture system was substantially worse than the coculture system with the isobutanol concentration decreasing 43 %

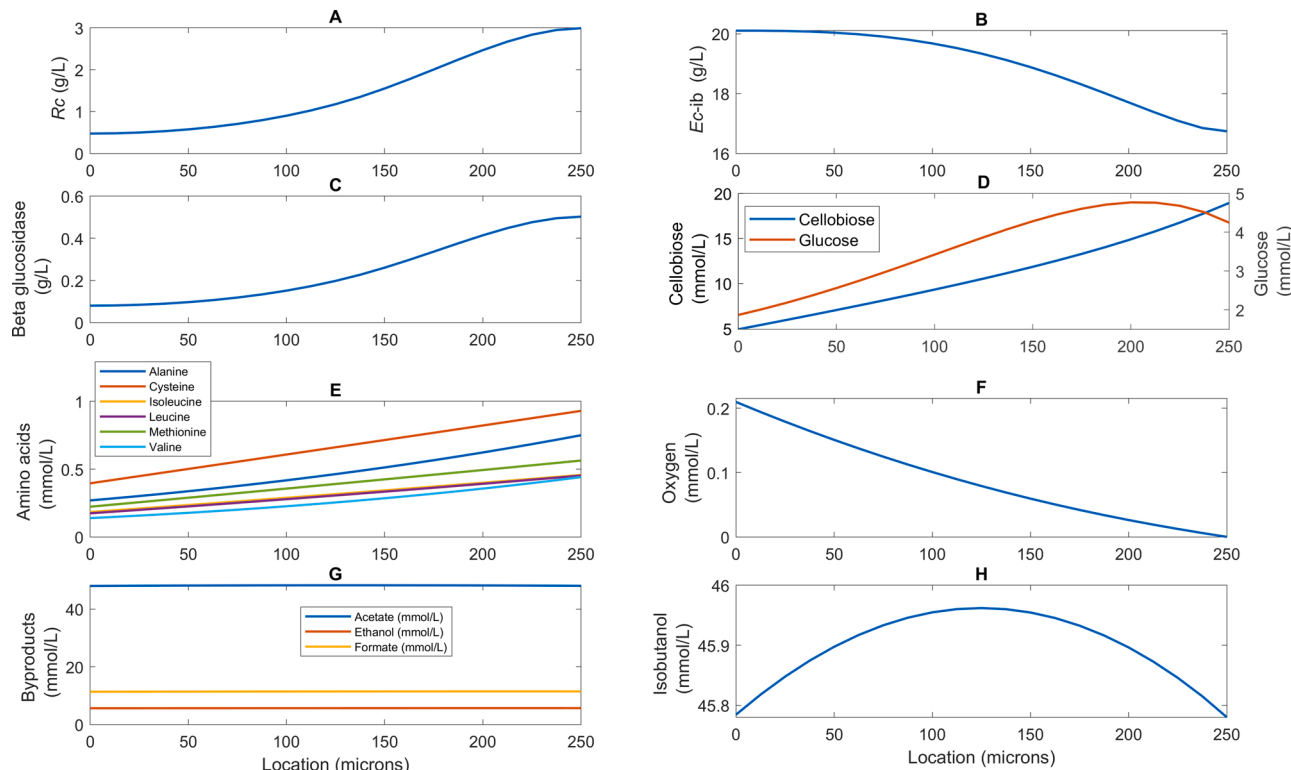


Fig. 2. Steady-state concentration profiles for coculture design 1 consisting of *Rc* and *Ec*-ib. (a) *Rc* biomass. (b) *Ec*-ib biomass. (c) β -glucosidase enzyme. (d) cellobiose and glucose. (e) six amino acids essential for *Rc* growth. (f) oxygen. (g) byproducts acetate, ethanol and formate. (h) isobutanol.

Table 1

Performance summary of community designs with different byproduct inhibition effects.

System	Acetate inhibition parameter (mmol/L)	Ethanol inhibition parameter (mmol/L)	Formate inhibition parameter (mmol/L)	Strain 1 mean biomass (g/L)	Strain 2 mean biomass (g/L)	Strain 3 mean biomass (g/L)	Isobutanol mean (mmol/L)
Rc, Ec-ib	80	600	400	1.5	18.9	—	45.9
Rc, Ec-ib	10^6	600	400	23.3	24.7	—	62.5
Rc, Ec-ib	80	10^6	400	1.5	19	—	46.02
Rc, Ec-ib	80	600	10^6	1.54	19	—	46.08
Rc, Ec-ib	10^6	10^6	10^6	26.6	40.8	—	97.1
Rc, Ec-ib, Ec-ac	80	600	400	23.15	10.61	19.13	26.34
Rc, Ec-ib, Gm	80	600	400	20.21	27.04	32.81	67.9
Cl, Ec-ib	80	600	400	0.67	29.1	—	50.43
Cl, Ec-ib	10^6	600	400	2.6	43.02	—	97.8
Cl, Ec-ib	80	10^6	400	0.67	29.21	—	50.6
Cl, Ec-ib	80	600	10^6	0.66	29.18	—	50.48
Cl, Ec-ib	10^6	10^6	10^6	2.69	43.35	—	99.01
Cl, Ec-ib, Ec-ac	80	600	400	0.84	59.66	11.23	64.6
Cl, Ec-ib, Gm	80	600	400	1.55	46.35	8.5	97.01

upon introduction of Ec-ac (Fig. 3). The desired alleviation of acetate inhibition was not achieved, as this triculture design suffered from deleterious interactions between the three strains that resulted in decreased Ec-ib biomass accumulation and therefore reduced isobutanol production. More specifically, Rc competed with Ec-ib for available glucose and Ec-ac competed with Ec-ib for O₂ to oxidize acetate. We attributed the substantially increased Rc biomass concentration (average of 23.2 g/L in triculture vs. 1.5 g/L in coculture) to reduced O₂ inhibition of Rc growth, which resulted in increased enzyme secretion and higher generation of growth-promoting glucose compared to cellobiose. Elevated Rc biomass resulted in higher production of both formate and ethanol, which collectively served to further suppress Ec-ib growth in the region near the membrane-biofilm interface (Fig. S2). The net result of these interactions was nonideal strain abundances, with the

biomass concentrations of both Rc and Ec-ac being too high compared to that of Ec-ib. These predictions yielded two general community design principles: 1) the cellulolytic bacterium should not strongly compete with the product-synthesizing bacterium for the primary substrate resulting from biopolymer degradation (e.g. glucose); and 2) the byproduct-consuming bacterium should not share an electron acceptor with the product-synthesizing bacterium (e.g. O₂).

3.3. R. chamarstellensis, isobutanol-producing E. coli and G. metallireducens system (Triculture design 2)

To investigate the possible advantages of using two different electron acceptors in the community design, we added acetate-consuming G. metallireducens (Gm) to the Rc/Ec-ib coculture (Fig. 1c). In this

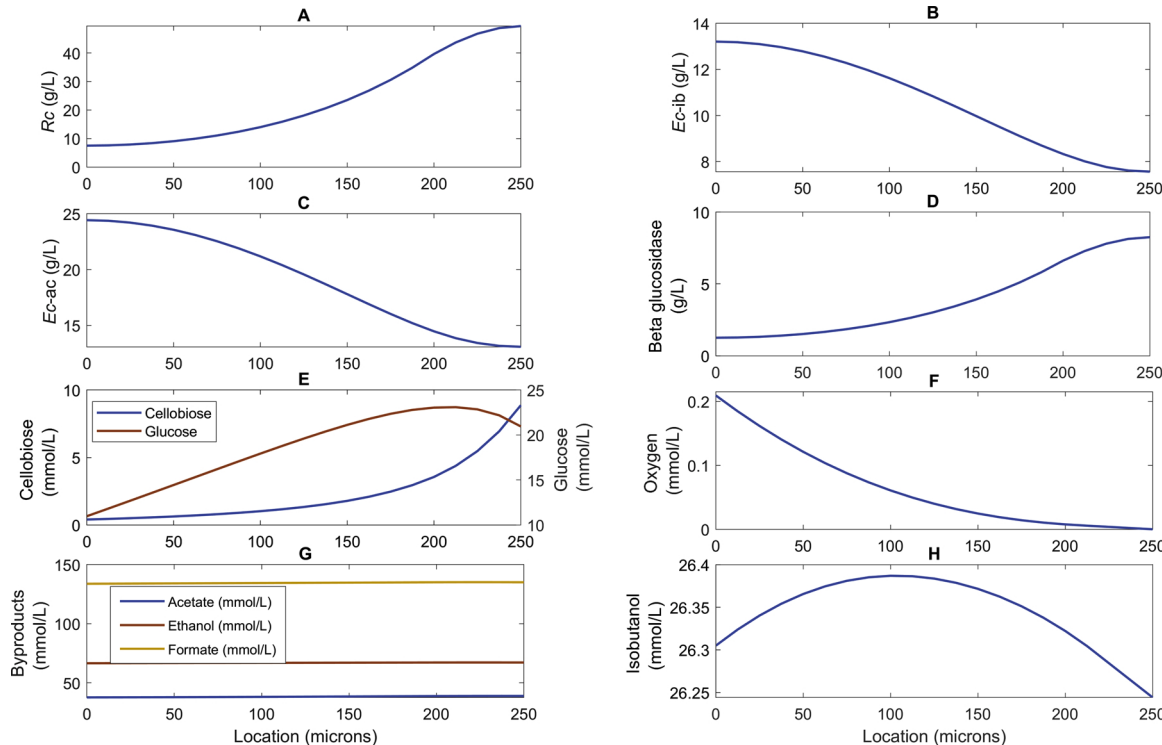


Fig. 3. Steady-state concentration profiles for triculture design 1 consisting of Rc, Ec-ib and Ec-ac. (a) Rc biomass. (b) Ec-ib biomass. (c) Ec-ac biomass. (d) β -glucosidase enzyme. (e) cellobiose and glucose. (f) oxygen. (g) byproducts acetate, ethanol and formate. (h) isobutanol.

triculture system, O_2 was only used by *Ec*-ib for microaerobic isobutanol production and Fe(III) was used by *Gm* as the terminal electron acceptor for anaerobic acetate oxidation. As expected, *Gm* accumulated preferentially in the O_2 -lean region near the membrane-biofilm interface where Fe(III) was supplied (Fig. 4). The isobutanol concentration was increased 158 % compared to the triculture design with *Ec*-ac and 48 % compared to the coculture system due to increased *Ec*-ib biomass accumulation. Interestingly, a major advantage of this triculture design was that *Ec*-ib had higher O_2 uptake near the surface (top?) (Fig. S3) and not that *Gm* was able to substantially reduce the concentration of inhibitory acetate. Flux balance analysis (FBA) predicted that *Gm* preferred to consume formate over acetate as its primary carbon source (not shown). The prediction of formate consumption by *Gm* was consistent with experimental observations [55], but we did not find any experimental studies that showed formate preference over acetate. While this triculture system offered increased O_2 availability for *Ec*-ib, isobutanol production was 30 % below the maximum value predicted when all byproduct inhibition effects were removed (Table 1). We concluded that the system design was limited by glucose competition between *Rc* and *Ec*-ib and acetate inhibition of *Ec*-ib growth. These predictions yielded a third community design principle: the byproduct-consuming bacterium should preferentially consume the byproduct primarily responsible for growth inhibition of the product-synthesizing bacterium (e.g. acetate).

3.4. *C. lentoceum* and isobutanol-producing *E. coli* system (Coculture design 2)

To test the robustness of the community behavior with an alternative cellulolytic bacterium, we replaced *Rc* with *C. lentoceum* (*Cl*) and performed biofilm simulations of the *Cl/Ec*-ib coculture system. The model predicted that *Cl* would only grow near the membrane-biofilm interface (Fig. S4), and therefore the *Cl* biomass concentration was lower than predicted for *Rc* in coculture (Fig. 5). Correspondingly, the average enzyme concentration was decreased and the glucose concentration remained low across the biofilm. Reduced utilization of glucose and synthesis of inhibitory byproducts (most notably formate) by *Cl* resulted

in higher total *Ec*-ib biomass, thereby reinforcing the design principle that consumption of the primary substrate must be balanced between the cellulolytic and product-synthesizing bacteria. Interestingly, *Ec*-ib biomass exhibited a peak near the middle of the biofilm where the combination of glucose and O_2 was most favorable for growth. Of the three amino acids essential for *in silico* *Cl* growth, alanine and glutamine were used by *Ec*-ib for growth enhancement. These various factors combined to generate a slightly higher isobutanol level than was predicted for the *Rc*-containing coculture. However, the isobutanol concentration for the *Cl/Ec*-ib coculture was only 51 % of the theoretical value predicted when the effects of all inhibitory byproducts was removed (Table 1), suggesting that introduction of a third bacterium capable of acetate consumption could substantially improve system performance.

3.5. *C. lentoceum*, isobutanol-producing *E. coli* and acetate-consuming *E. coli* system (Triculture design 3)

Next simulations were performed for the triculture system obtained by adding the acetate consumer *Ec*-ac to the *Cl/Ec*-ib coculture biofilm. While *Ec*-ib competed with *Cl* for glucose and with *Ec*-ac for O_2 , the *Cl* biomass concentration remained low such that sufficient glucose was available to support *Ec*-ib growth (Fig. 6). Additionally, acetate secreted by *Cl* and *Ec*-ib as their primary byproduct was mostly consumed by *Ec*-ac such that the acetate concentration was 12 mmol/L, well below the maximum inhibitory value of 80 mmol/L. These two effects combined to allow the average *Ec*-ib biomass concentration to approach 60 g/L and the isobutanol concentration to reach 65 mmol/L, a 28 % increase over the *Cl/Ec*-ib coculture value (Table 1). Moderate O_2 consumption in the upper half of the biofilm resulted in an O_2 profile that created a large region supporting *Ec*-ib and *Ec*-ac growth and a much smaller anaerobic region supporting *Cl* growth (Fig. S5). While the disadvantages of strong glucose competition and formate production by *Rc* (which resulted in inhibitory acetate levels due to preferential formate consumption by *Gm*) that plagued the *Rc*-containing tricultures were eliminated, this *Cl*-containing triculture system still suffered from O_2 competition between

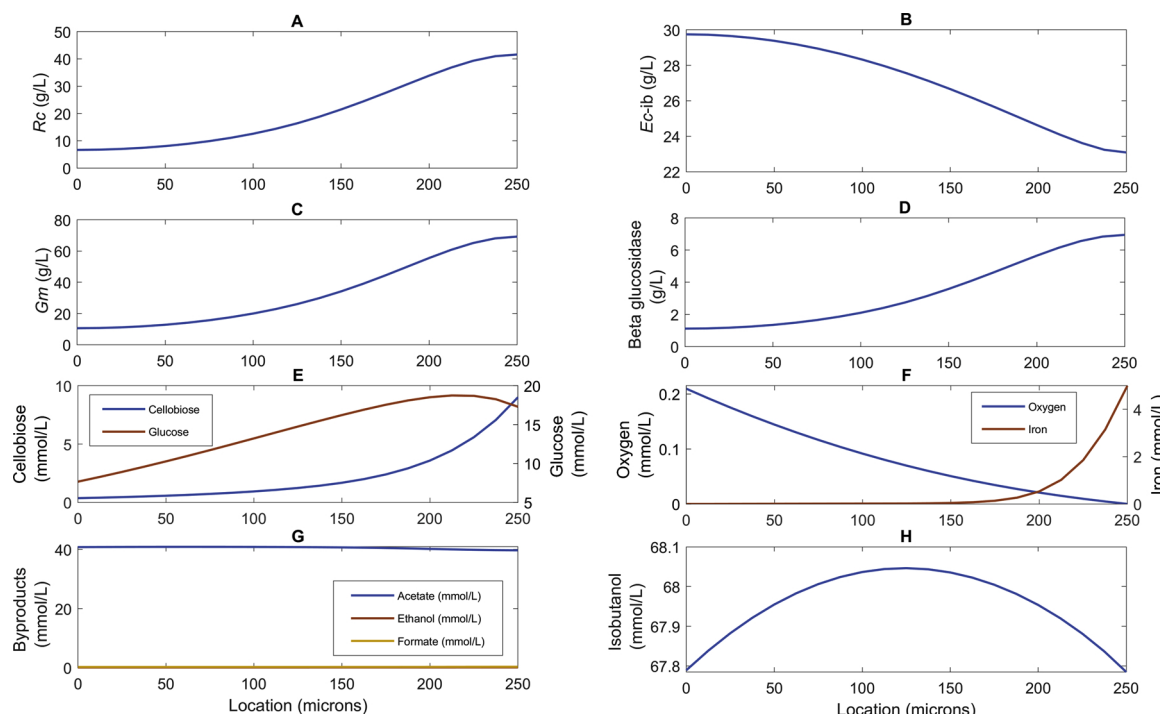


Fig. 4. Steady-state concentration profiles for triculture design 2 consisting of *Rc*, *Ec*-ib and *Gm*. (a) *Rc* biomass. (b) *Ec*-ib biomass. (c) *Gm* biomass. (d) β -glucosidase enzyme. (e) cellobiose and glucose. (f) oxygen and iron. (g) byproducts acetate, ethanol and formate. (h) isobutanol.

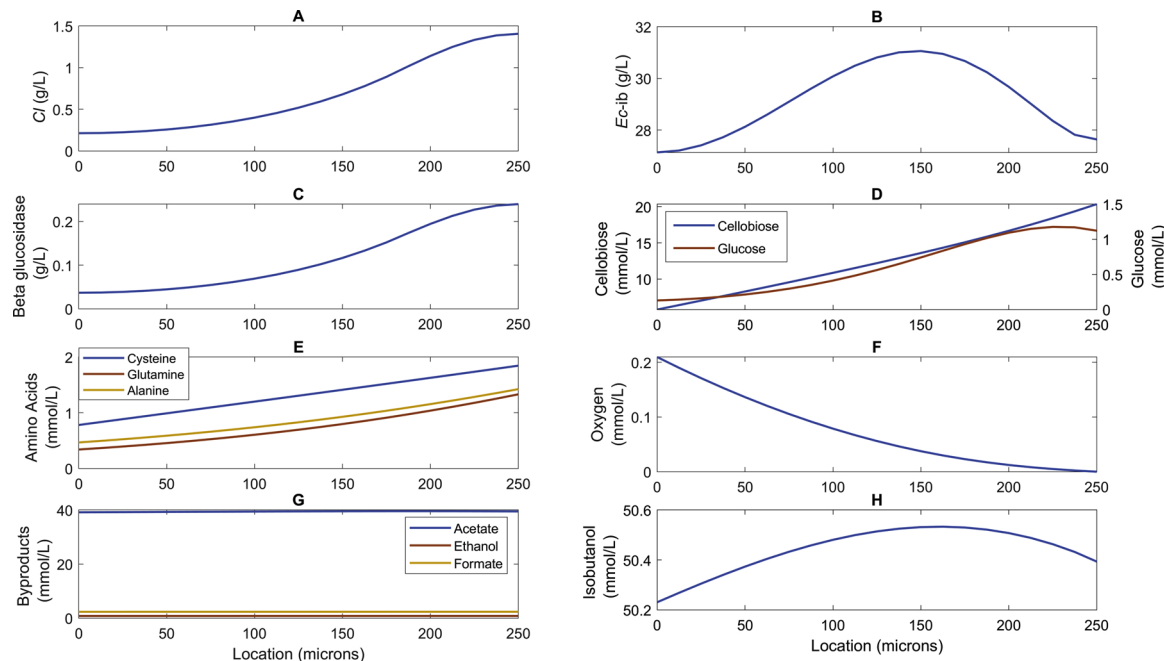


Fig. 5. Steady-state concentration profiles for coculture design 2 consisting of Cl and $Ec\text{-ib}$. (a) Cl biomass. (b) $Ec\text{-ib}$ biomass. (c) β -glucosidase enzyme. (d) cellulose and glucose. (e) three amino acids essential for Cl growth. (f) oxygen. (g) byproducts acetate, ethanol and formate. (h) isobutanol.

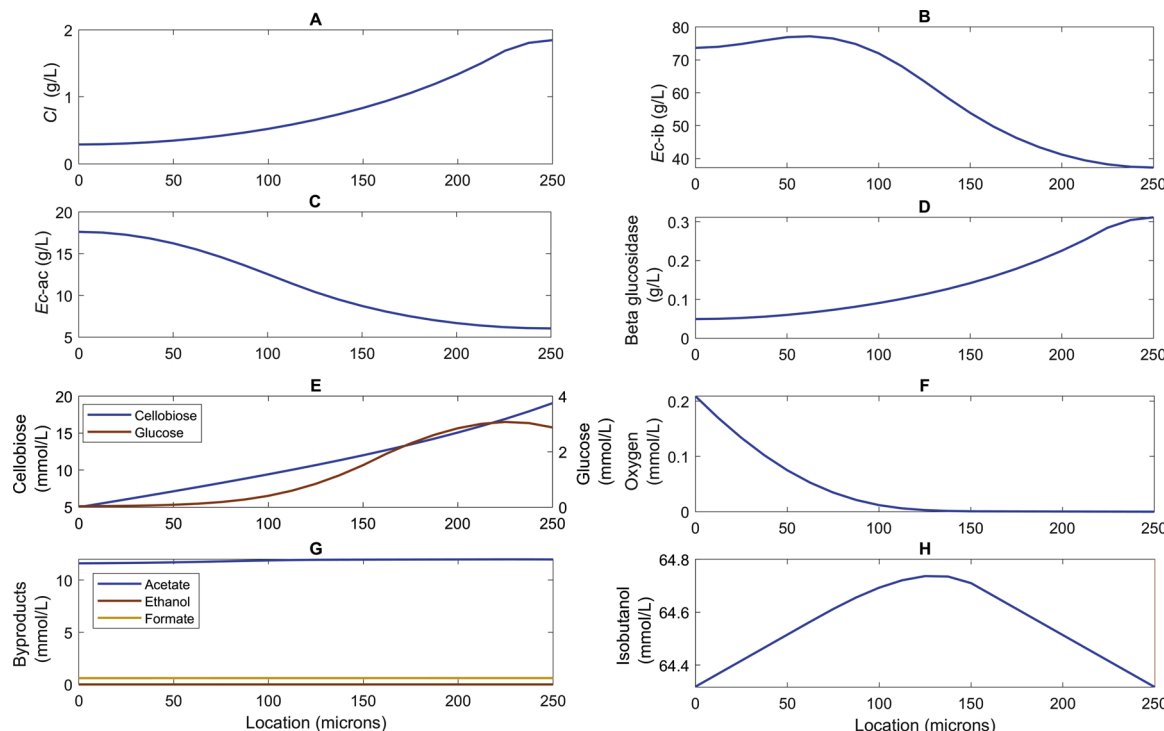


Fig. 6. Steady-state concentration profiles for triculture design 3 consisting of Cl , $Ec\text{-ib}$ and $Ec\text{-ac}$. (a) Cl biomass. (b) $Ec\text{-ib}$ biomass. (c) $Ec\text{-ac}$ biomass. (d) β -glucosidase enzyme. (e) cellulose and glucose. (f) oxygen. (g) byproducts acetate, ethanol and formate. (h) isobutanol.

the two *E. coli* strains as demonstrated by the isobutanol concentration being only 65 % of the value when all byproduct inhibitions were removed (Table 1).

3.6. *C. lentoceum*, isobutanol-producing *E. coli* and acetate-consuming *G. metallireducens* system (Triculture design 4)

We hypothesized that replacement of aerobic $Ec\text{-ac}$ with anaerobic

Gm to eliminate O_2 competition would have two benefits: 1) acetate consumption would not be limited by O_2 availability and therefore the acetate inhibition effect could be almost entirely eliminated; and 2) more O_2 would be available to support $Ec\text{-ib}$ growth and isobutanol synthesis. The triculture design was predicted to provide the first benefit as Gm reduced the average acetate concentration to 1 mmol/L, almost completely eliminating byproduct inhibition of the other two strains (Fig. 7). As a result, Cl biomass accumulation, enzyme synthesis and

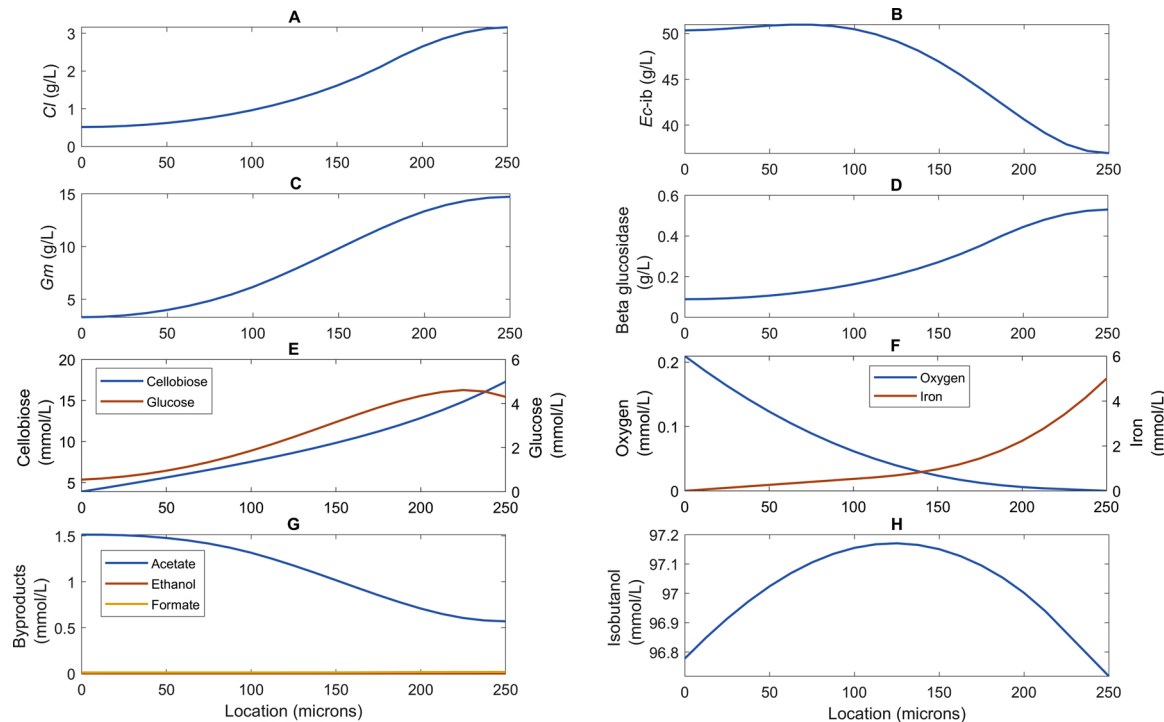


Fig. 7. Steady-state concentration profiles for triculture design 3 consisting of *Cl*, *Ec-ib* and *Gm*. (a) *Cl* biomass. (b) *Ec-ib* biomass. (c) *Gm* biomass. (d) β -glucosidase enzyme. (e) cellobiose and glucose. (f) oxygen. (g) byproducts acetate, ethanol and formate. (h) isobutanol.

glucose availability all increased in unison. The hypothesized O_2 availability benefit was more complex than anticipated, as the isobutanol concentration was increased but *Ec-ib* biomass accumulation actually decreased compared to the other *Cl*-containing triculture design. This apparent inconsistency was rationalized by a more moderate O_2 concentration profile allowing high isobutanol production across a larger region of the biofilm (compare Figs. S5 and S6). More precisely, the glucose and O_2 uptakes across the biofilm combined to produce

microaerobic growth conditions that promoted isobutanol synthesis over biomass accumulation. As a result, this *Cl/Ec-ib/Gm* triculture design was predicted to achieve an isobutanol concentration within 2% of the value calculated in the absence of byproduct inhibitions (Table 1). While these results were not easily encapsulated in a simple community design principle, the value of having rigorous metabolic models to predict biofilm behavior as a function of participating strains and supplied nutrients was readily apparent.

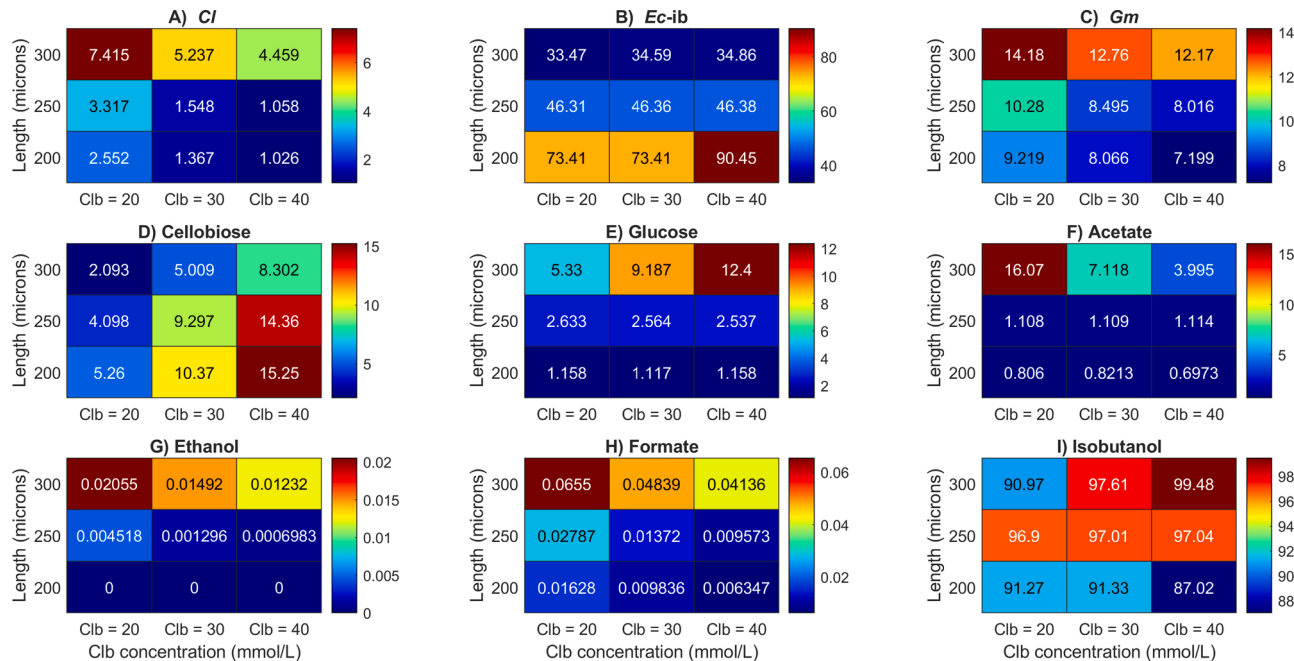


Fig. 8. Steady-state concentrations average across the biofilm for nine combinations of the supplied cellobiose concentration (Clb) and biofilm thickness for triculture design 4 consisting of *Cl*, *Ec-ib* and *Gm*. (a) *Cl* biomass. (b) *Ec-ib* biomass. (c) *Gm* biomass. (d) cellobiose. (e) glucose. (f) acetate. (g) ethanol. (h) formate. (i) isobutanol.

3.7. Stability and robustness of community system designs

We investigated robustness of the four triculture designs for nine combinations of the cellobiose supply concentration (20, 30, 40 mmol/L) and the biofilm height (200, 250, 300 µm) as a means to examine their stability (*i.e.* coexistence of the three strains) and performance (*i.e.* isobutanol concentration). The base case for our analysis corresponded to the nominal conditions (30 mmol/L cellobiose, 250 µm thickness) used to generate all the previous simulation results. A design was termed “robust” if the three strains coexisted over the entire range of conditions and the isobutanol concentration did not decrease more than 20 % from the base case value at any one condition.

According to this definition, the *Ct/Ec-ib/Gm* triculture system was particularly robust as the three strains retained relative abundances such that the isobutanol concentration decreased no more than 11 % (Fig. 8). Thicker biofilms favored the growth of *Ct* and *Gm* compared to *Ec-ib* because a larger anaerobic region was created. As a result, thicker biofilms were predicted to have reduced free cellobiose but increased unconsumed glucose. Unconsumed acetate increased in thicker biofilms due to limitations in the flux of Fe(III). As the cellobiose concentration was increased, *Ct* biomass decreased due to an increased growth penalty for enzyme synthesis, *Ec-ib* biomass remained almost constant (except for one case) due to limited O₂ availability and *Gm* biomass decreased due to reduced acetate availability. Correspondingly, free cellobiose and unconsumed glucose both increased with increasing cellobiose supply. These various effects combined to generate high isobutanol concentrations at all conditions with slight decreases predicted at large height, low cellobiose due to acetate inhibition and at small height, high cellobiose due to an unfavorable O₂ profile across the biofilm.

When evaluated for the same combination of conditions, the other three triculture designs were robustly stable in the sense that the three participating strains coexisted at all conditions. The *Ct/Ec-ib/Ec-ac* system was predicted to be particularly robust as the isobutanol concentration decreased less than 1 % across the non-base case conditions despite substantial variations in the biomass concentrations of the three strains, most notably *Ec-ib* (Fig. S7). The two *Rc*-containing communities were predicted to exhibit larger isobutanol variations. For example, the *Rc/Ec-ib/Gm* system was particularly sensitive to the biofilm thickness, with thinner biofilms favoring *Ec-ib* biomass accumulation and generating isobutanol concentrations approaching those of the *Ct/Ec-ib/Gm* system (Fig. S8). The *Rc/Ec-ib/Ec-ac* system was predicted to generate reasonable isobutanol concentrations only for the thinnest biofilms (Fig. S9), and even those concentrations were well below values for *Ct/Ec-ib/Gm* system.

To explore the impact of metabolic redundancy on compositional stability, we performed biofilm simulations with all five strains (*Rc*, *Ct*, *Ec-ib*, *Gm* and *Ec-ac*) included in the community. While *Ec-ib* continued to serve the unique role of isobutanol producer, *Rc* and *Ct* offered redundant cellobiose degradation capabilities and *Gm* and *Ec-ac* offered redundant acetate consumption capabilities. The *in silico* media used for these five-strain simulations included the seven amino acids required for *Rc* and *Ct* growth. Due to its more rapid growth, *Rc* outcompeted *Ct* for cellobiose and glucose. The availability of the unique electron acceptor Fe(III) allowed *Gm* to more rapidly consume acetate than *Ec-ac*, which had to compete for O₂ with *Ec-ib* (Figs. S10 and S11). Consequently, both *Ct* and *Ec-ac* were unable to coexist and a three-species community consisting of *Rc*, *Ec-ib* and *Gm* resulted. These predictions generated a fourth community design principle: excessive metabolic redundancy between community members can result in loss of compositional stability and extinction of less competitive members.

4. Discussion

Synthetic biofilm communities hold considerable promise for biotechnological applications due to their ability to robustly accommodate bacteria with different, but complementary metabolisms that

allow complex bioconversions. In this paper, we used *in silico* metabolic modeling to explore the design of synthetic communities for conversion of the plant-derived disaccharide cellobiose to the important platform chemical isobutanol. In addition to proposing specific community designs for this problem, we sought to use this model system to develop general design principles that could be applicable to a wide range of bioconversion tasks. Following the microbial ecology principle of division of labor, our *in silico* communities consisted of three specialist bacteria: 1) a cellulolytic anaerobe which secreted the enzyme β-glucosidase for cleavage of cellobiose to two glucose monomers; 2) an microaerobic isobutanol producer which converted free glucose to the desired product; and 3) an aerobic or anaerobic byproduct consumer which scavenged secreted organic acids that inhibited the growth of the other two strains. We performed biofilm simulations of the four distinct communities that paired an isobutanol-producing *Escherichia coli* (*Ec-ib*) mutant with different cellulolytic gut bacteria (*Ruminococcus channellensis* (*Rc*) or *Cellulosilyticum lentocellum* (*Ct*)) and byproduct consumers (anaerobic *Geobacter metallireducens* (*Gm*) or an aerobic acetate-consuming *E. coli* mutant (*Ec-ac*)).

To provide a basis for assessing the contributions of the byproduct consumers, we first simulated the *Rc/Ec-ib* and *Ct/Ec-ib* coculture systems. The cellulolytic bacteria *Rc* and *Ct* had different growth phenotypes, with *Ct* consuming less glucose and growing more slowly and *Rc* producing large amounts of formate in addition to acetate. The two coculture systems were predicted to generate similar isobutanol concentrations (45–50 mmol/L), with the *Ct/Ec-ib* system providing slightly better performance due to greater glucose availability and less acetate-induced inhibition of growth. These metabolic differences proved to be more impactful when byproduct consumers were added to form the four triculture biofilm systems.

The *Ec-ac* mutant was specifically engineered to aerobically metabolize acetate without consuming glucose [15]. While *Ec-ac* did not compete with *Ec-ib* for glucose, the two *E. coli* mutants did compete for limited O₂. Furthermore, *Ec-ib* competed for free glucose with the cellulolytic bacteria, and *Ec-ac* was not capable of consuming organic acids other than acetate. Therefore, the *Rc/Ec-ib/Ec-ac* triculture system suffered from several shortcomings that inherently restricted isobutanol production: 1) *Ec-ib* competition with *Rc* for the electron donor glucose and with *Ec-ac* for the electron acceptor O₂ combined to limit *Ec-ib* biomass accumulation; and 2) formate secreted by *Rc* was not consumed by *Ec-ac*, resulting in growth inhibition of *Rc* and *Ec-ib*. This triculture design was predicted to be the least productive for the nominal biofilm parameters, generating an isobutanol concentration only 43 % of the *Rc/Ec-ib* coculture value. Improved performance was predicted for thinner biofilms with a smaller anaerobic region for *Rc* growth, reducing glucose competition and formate inhibition.

We hypothesized that replacement of *Ec-ac* with *Gm* would improve system performance by eliminating O₂ competition, as *Gm* used Fe(III) as its terminal electron acceptor, and by reducing formate levels, as *Gm* was capable of metabolizing both formate and acetate. Indeed, for the nominal biofilm parameters the *Rc/Ec-ib/Gm* triculture increased the isobutanol concentration 48 % compared to the coculture system. However, *Gm* exhibited a preference for formate rather than acetate as a carbon source and therefore failed to substantially reduce acetate inhibition of *Rc* and *Ec-ib*. System performance was predicted to be strongly dependent on biofilm thickness, with thinner biofilms reducing formate secretion by *Rc* and allowing more acetate consumption. Because our models use biofilm thickness as an input parameter, we cannot actually predict how the thickness could be adjusted. However, the formation of thinner biofilms could be achieved by reducing the supplied cellobiose concentration.

Selection of an appropriate cellulolytic bacterium represented a compromise between cellobiose degradation, as the isobutanol producer required glucose for growth, and cellobiose/glucose consumption, as the cellulolytic organism required these carbon sources for growth and synthesis of the β-glucosidase. We replaced *Rc* with *Ct* to determine if

triculture performance could be improved by incorporating a cellulolytic bacterium with slower growth, reduced glucose consumption and limited formate production. Indeed, the *Ct/Ec-ib/Ec-ac* system was predicted to outperform the corresponding *Rc*-containing triculture by generating a 146 % higher isobutanol concentration for the nominal biofilm parameters. System performance was almost independent of the biofilm height and cellobiose supply concentration, suggesting a very robust design. However, isobutanol production remained limited by O₂ competition between *Ec-ib* and *Ec-ac*.

By replacing *Ec-ac* with *Gm* to eliminate O₂ competition, we obtained the top performing triculture which generated an isobutanol concentration 43 % higher than the second best design (*Rc/Ec-ib/Gm*). The *Ct/Ec-ib/Gm* biofilm system possessed several key properties that promoted high product synthesis: 1) the average *Ct* cell density across the biofilm was high enough to produce sufficient enzyme but low enough to leave most free glucose for *Ec-ib* consumption; 2) *Ct* secreted acetate at its primary byproduct and *Gm* consumed acetate as its only carbon source such that organic acid-induced growth inhibition was effectively eliminated; and 3) *Ec-ib* was able to secrete isobutanol across a large region of the biofilm due to complementary glucose and O₂ profiles which created microaerobic growth conditions. This system design also was predicted to be very robust as the isobutanol concentration decreased only 10 % when a relatively small biofilm thickness and high cellobiose concentration combined to reduce the microaerobic region.

5. Conclusion

We used *in silico* metabolic modeling to investigate the stability, performance and robustness of three-strain, biofilm systems for conversion of cellobiose to isobutanol. The four systems tested were comprised of a mutant *E. coli* strain engineered for glucose-to-isobutanol conversion paired with a cellulolytic, gut bacterium for extracellular cellulose-to-glucose degradation and a byproduct consumer for scavenging of growth-inhibiting organic acids. While all four tricultures were predicted to be stable, we found that system performance was strongly dependent on metabolic interactions between the three strains. Our biofilm simulations revealed the following design principles that could guide selection of compatible community members:

- 1 The cellulolytic organism should be chosen to achieve a compromise between undesirable monomer competition with the product-synthesizing organism and sufficient enzyme synthesis for monomer generation.
- 2 The product-synthesizing and byproduct-consuming organisms should not compete for the same terminal electron acceptor.
- 3 The byproduct-consuming organism should be matched with the cellulolytic and product-synthesizing organisms according to byproduct crossfeeding with the most inhibitory byproduct serving as the preferred carbon source of the byproduct consumer.
- 4 Excessive metabolic redundancy between community members can result in loss of compositional stability and extinction of less competitive members.

Of the four systems designs investigated, the community consisting of cellulolytic *Cellulosilyticum lentocellum* and byproduct-consuming *Geobacter metallireducens* paired with isobutanol-producing *E. coli* generated the highest isobutanol concentrations across a range of biofilm model parameters. This system satisfied the three community design principles listed above including: 1) *C. lentocellum* secreted sufficient enzyme for glucose generation but maintained a sufficiently low cell density to allow most free glucose to be consumed by the *E. coli* mutant; 2) *G. metallireducens* utilized Fe(III) as its electron acceptor while the *E. coli* mutant was the only organisms requiring O₂; and 3) *C. lentocellum* and the *E. coli* mutant both secreted acetate at their primary byproduct and *G. metallireducens* readily consumed as acetate as its primary carbon source. In addition to generating a promising triculture

biofilm system suitable for future experimental testing and optimization, we believe that these design principles will have broad applicability to synthetic microbial communities developed for other biotechnological applications.

Declaration of Competing Interest

The authors report no declarations of interest.

Acknowledgments

This work was supported by NSF Award 2030087 (https://www.nsf.gov/awardsearch/showAward?AWD_ID=2030087).

Appendix A. Supplementary data

Supplementary material related to this article can be found, in the online version, at doi:<https://doi.org/10.1016/j.bej.2021.108032>.

References

- [1] B. Rosche, X.Z. Li, B. Hauer, A. Schmid, K. Buehler, Microbial biofilms: a concept for industrial catalysis? *Trends Biotechnol.* 27 (2009) 636–643.
- [2] N. Qureshi, B.A. Annous, T.C. Ezeji, P. Karcher, I.S. Maddox, Biofilm reactors for industrial bioconversion processes: employing potential of enhanced reaction rates, *Microb. Cell Fact.* 4 (2005) 24.
- [3] J. Shong, M.R.J. Diaz, C.H. Collins, Towards synthetic microbial consortia for bioprocessing, *Curr. Opin. Biotechnol.* 23 (2012) 798–802.
- [4] A. Mohagheghi, K. Grohmann, C.E. Wyman, Production of cellulase on mixtures of xylose and cellulose, *Appl. Biochem. Biotechnol.* 17 (1988) 263–277.
- [5] G. Bokinsky, P.P. Peralta-Yahya, A. George, B.M. Holmes, E.J. Steen, J. Dietrich, T. S. Lee, D. Tullman-Ercek, C.A. Voigt, B.A. Simmons, Synthesis of three advanced biofuels from ionic liquid-pretreated switchgrass using engineered *Escherichia coli*, *Proc. Natl. Acad. Sci.* 108 (2011) 19949–19954.
- [6] K.M. Smith, K.-M. Cho, J.C. Liao, Engineering *Corynebacterium glutamicum* for isobutanol production, *Appl. Microbiol. Biotechnol.* 87 (2010) 1045–1055.
- [7] C.T. Trinh, J. Li, H.W. Blanch, D.S. Clark, Redesigning *Escherichia coli* metabolism for anaerobic production of isobutanol, *Appl. Environ. Microbiol.* 77 (2011) 4894–4904.
- [8] J.H. Lee, S. Lama, J.R. Kim, S.H. Park, Production of 1, 3-propanediol from glucose by recombinant *Escherichia coli* BL21 (DE3), *Biotechnol. Bioprocess Eng.* 23 (2018) 250–258.
- [9] C.J. Frazão, D. Trichez, H. Serrano-Bataille, A. Dagkesamanskaya, C.M. Topham, T. Walther, J.M. François, Construction of a synthetic pathway for the production of 1, 3-propanediol from glucose, *Sci. Rep.* 9 (2019) 1–12.
- [10] G.W. Roell, J. Zha, R.R. Carr, M.A. Koffas, S.S. Fong, Y.J. Tang, Engineering microbial consortia by division of labor, *Microb. Cell Fact.* 18 (2019) 35.
- [11] I.-T. Tong, H.H. Liao, D.C. Cameron, 1, 3-Propanediol production by *Escherichia coli* expressing genes from the *Klebsiella pneumoniae* dha regulon, *Appl. Environ. Microbiol.* 57 (1991) 3541–3546.
- [12] K. Brenner, L. You, F.H. Arnold, Engineering microbial consortia: a new frontier in synthetic biology, *Trends Biotechnol.* 26 (2008) 483–489.
- [13] T.R. Zuroff, W.R. Curtis, Developing symbiotic consortia for lignocellulosic biofuel production, *Appl. Microbiol. Biotechnol.* 93 (2012) 1423–1435.
- [14] P. Moens, C.W. Michiels, A. Aertsen, Bacterial interactions in biofilms, *Crit. Rev. Microbiol.* 35 (2009) 157–168.
- [15] H.C. Bernstein, S.D. Paulson, R.P. Carlson, Synthetic *Escherichia coli* consortia engineered for syntropy demonstrate enhanced biomass productivity, *J. Biotechnol.* 157 (2012) 159–166.
- [16] A. Briones, L. Raskin, Diversity and dynamics of microbial communities in engineered environments and their implications for process stability, *Curr. Opin. Biotechnol.* 14 (2003) 270–276.
- [17] D.G. Olson, J.E. McBride, A.J. Shaw, L.R. Lynd, Recent progress in consolidated bioprocessing, *Curr. Opin. Biotechnol.* 23 (2012) 396–405.
- [18] S. Kondo, T. Miura, Reaction-diffusion model as a framework for understanding biological pattern formation, *Science* 329 (2010) 1616–1620.
- [19] M.R. Kunduru, A. Pometto, Continuous ethanol production by *Zymomonas mobilis* and *Saccharomyces cerevisiae* in biofilm reactors, *J. Ind. Microbiol.* 16 (1996) 249–256.
- [20] S. Brethauer, M.H. Studer, Consolidated bioprocessing of lignocellulose by a microbial consortium, *Energy Environ. Sci.* 7 (2014) 1446–1453.
- [21] M. Wagner, A. Loy, Bacterial community composition and function in sewage treatment systems, *Curr. Opin. Biotechnol.* 13 (2002) 218–227.
- [22] A.F. Miranda, N. Ramkumar, C. Andriotis, T. Höltkemeier, A. Yasmin, S. Rochfort, D. Włodkowic, P. Morrison, F. Roddick, G. Spangenberg, Applications of microalgal biofilms for wastewater treatment and bioenergy production, *Biotechnol. Biofuels* 10 (2017) 120.
- [23] F. Gebara, Activated sludge biofilm wastewater treatment system, *Water Res.* 33 (1999) 230–238.

- [24] B. Capdeville, J. Rols, Introduction to biofilms in water and wastewater treatment. *Biofilms—Science and Technology*, Springer, 1992, pp. 13–20.
- [25] Y. Qu, Y. Feng, X. Wang, B.E. Logan, Use of a coculture to enable current production by *Geobacter sulfurreducens*, *Appl. Environ. Microbiol.* 78 (2012) 3484–3487.
- [26] Z. Ren, L. Steinberg, J. Regan, Electricity production and microbial biofilm characterization in cellulose-fed microbial fuel cells, *Water Sci. Technol.* 58 (2008) 617–622.
- [27] S.T. Read, P. Dutta, P.L. Bond, J. Keller, K. Rabaey, Initial development and structure of biofilms on microbial fuel cell anodes, *BMC Microbiol.* 10 (2010) 98.
- [28] A. Buetti-Dinh, V. Galli, S. Bellenberg, O. Ilie, M. Herold, S. Christel, M. Boretska, I. V. Pivkin, P. Wilmes, W. Sand, Deep neural networks outperform human expert's capacity in characterizing bioleaching bacterial biofilm composition, *Biotechnol. Rep.* 22 (2019), e00321.
- [29] Z.-W. Wang, S. Chen, Potential of biofilm-based biofuel production, *Appl. Microbiol. Biotechnol.* 83 (2009) 1–18.
- [30] S.J. Lee, T.A. Warnick, S. Pattathil, J.G. Alvelo-Maurosa, M.J. Serapiglia, H. McCormick, V. Brown, N.F. Young, D.J. Schnell, L.B. Smart, Biological conversion assay using *Clostridium phytofermentans* to estimate plant feedstock quality, *Biotechnol. Biofuels* 5 (2012) 5.
- [31] X. Wu, J. McLaren, R. Madl, D. Wang, Biofuels from lignocellulosic biomass. *Sustainable Biotechnology*, Springer, 2010, pp. 19–41.
- [32] J.J. Minty, M.E. Singer, S.A. Scholz, C.-H. Bae, J.-H. Ahn, C.E. Foster, J.C. Liao, X. N. Lin, Design and characterization of synthetic fungal-bacterial consortia for direct production of isobutanol from cellulosic biomass, *Proc. Natl. Acad. Sci. U. S. A.* 110 (2013) 14592–14597.
- [33] K. Chomvong, V. Kordić, X. Li, S. Bauer, A.E. Gillespie, S.-J. Ha, E.J. Oh, J. M. Galazka, Y.-S. Jin, J.H. Cate, Overcoming inefficient cellobiose fermentation by cellobiose phosphorylase in the presence of xylose, *Biotechnol. Biofuels* 7 (2014) 85.
- [34] T.R. Zuroff, S.B. Xiques, W.R. Curtis, Consortia-mediated bioprocessing of cellulose to ethanol with a symbiotic *Clostridium phytofermentans*/yeast co-culture, *Biotechnol. Biofuels* 6 (2013) 59.
- [35] D. Weuster-Botz, A. Aivasidis, C. Wandrey, Continuous ethanol production by *Zymomonas mobilis* in a fluidized bed reactor. Part II: process development for the fermentation of hydrolysed B-starch without sterilization, *Appl. Microbiol. Biotechnol.* 39 (1993) 685–690.
- [36] S. Zhang, O. Norrlöw, J. Wawrzynczyk, E.S. Dey, Poly (3-hydroxybutyrate) biosynthesis in the biofilm of *Alcaligenes eutrophus*, using glucose enzymatically released from pulp fiber sludge, *Appl. Environ. Microbiol.* 70 (2004) 6776–6782.
- [37] J. Van Grootenhuis, J. Geelhoed, H. Gooris, K. Meesters, A. Stams, P. Claassen, Performance and population analysis of a non-sterile trickle bed reactor inoculated with *Caldicellulosiruptor saccharolyticus*, a thermophilic hydrogen producer, *Biotechnol. Bioeng.* 102 (2009) 1361–1367.
- [38] X.Z. Li, J.S. Webb, S. Kjelleberg, B. Rosche, Enhanced benzaldehyde tolerance in *Zymomonas mobilis* biofilms and the potential of biofilm applications in fine-chemical production, *Appl. Environ. Microbiol.* 72 (2006) 1639–1644.
- [39] B. Zhou, G.J. Martin, N.B. Pamment, Increased phenotypic stability and ethanol tolerance of recombinant *Escherichia coli* KO11 when immobilized in continuous fluidized bed culture, *Biotechnol. Bioeng.* 100 (2008) 627–633.
- [40] M.A. Henson, T.J. Hanly, Dynamic flux balance analysis for synthetic microbial communities, *IET Syst. Biol.* 8 (2014) 214–229.
- [41] K.S. Ang, M. Lakshmanan, N.-R. Lee, D.-Y. Lee, Metabolic modeling of microbial community interactions for health, environmental and biotechnological applications, *Curr. Genomics* 19 (2018) 712–722.
- [42] E. Bosi, G. Bacci, A. Mengoni, M. Fondi, Perspectives and challenges in microbial communities metabolic modeling, *Front. Genet.* 8 (2017) 88.
- [43] M. Hanemaijer, W.F. Röling, B.G. Olivier, R.A. Khandelwal, B. Teusink, F. J. Bruggeman, Systems modeling approaches for microbial community studies: from metagenomics to inference of the community structure, *Front. Microbiol.* 6 (2015) 213.
- [44] X. Li, M.A. Henson, Metabolic modeling of bacterial co-culture systems predicts enhanced carbon monoxide-to-butyrate conversion compared to monoculture systems, *Biochem. Eng. J.* 151 (2019), 107338.
- [45] A. Patel, R.P. Carlson, M.A. Henson, In silico metabolic design of two-strain biofilm systems predicts enhanced biomass production and biochemical synthesis, *Biotechnol. J.* (2019), 1800511.
- [46] J. Chen, J.A. Gomez, K. Höffner, P. Phalak, P.I. Barton, M.A. Henson, Spatiotemporal modeling of microbial metabolism, *BMC Syst. Biol.* 10 (2016) 21.
- [47] M.A. Henson, P. Phalak, Byproduct cross feeding and community stability in an in silico biofilm model of the gut microbiome, *Processes* 5 (2017) 13.
- [48] P. Phalak, J. Chen, R.P. Carlson, M.A. Henson, Metabolic modeling of a chronic wound biofilm consortium predicts spatial partitioning of bacterial species, *BMC Syst. Biol.* 10 (2016) 90.
- [49] R.P. Carlson, A.E. Beck, P. Phalak, M.W. Fields, T. Gedeon, L. Hanley, W. R. Harcombe, M.A. Henson, J.J. Heys, Competitive resource allocation to metabolic pathways contributes to overflow metabolisms and emergent properties in cross-feeding microbial consortia, *Biochem. Soc. Trans.* 46 (2018) 269–284.
- [50] S. Li, J. Wen, X. Jia, Engineering *Bacillus subtilis* for isobutanol production by heterologous Ehrlich pathway construction and the biosynthetic 2-ketoisovalerate precursor pathway overexpression, *Appl. Microbiol. Biotechnol.* 91 (2011) 577–589.
- [51] S. Atsumi, T. Hanai, J.C. Liao, Non-fermentative pathways for synthesis of branched-chain higher alcohols as biofuels, *Nature* 451 (2008) 86.
- [52] P.P. Peralta-Yahya, F. Zhang, S.B. Del Cardayre, J.D. Keasling, Microbial engineering for the production of advanced biofuels, *Nature* 488 (2012) 320–328.
- [53] C.-T. Chen, J.C. Liao, Frontiers in microbial 1-butanol and isobutanol production, *FEMS Microbiol. Lett.* 363 (2016) fnw020.
- [54] A.M. Feist, C.S. Henry, J.L. Reed, M. Krummenacker, A.R. Joyce, P.D. Karp, L. J. Broadbelt, V. Hatzimanikatis, B.Ø. Palsson, A genome-scale metabolic reconstruction for *Escherichia coli* K-12 MG1655 that accounts for 1260 ORFs and thermodynamic information, *Mol. Syst. Biol.* 3 (2007) 121.
- [55] A.M. Feist, H. Nagarajan, A.-E. Rotaru, P.-L. Tremblay, T. Zhang, K.P. Nevin, D. R. Lovley, K. Zengler, Constraint-based modeling of carbon fixation and the energetics of electron transfer in *Geobacter metallireducens*, *PLoS Comput. Biol.* 10 (2014), e1003575.
- [56] C. Guilhen, C. Forestier, D. Balestreno, Biofilm dispersal: multiple elaborate strategies for dissemination of bacteria with unique properties, *Mol. Microbiol.* 105 (2017) 188–210.
- [57] N. Allocati, M. Masulli, C. Di Ilio, V. De Laurenzi, Die for the community: an overview of programmed cell death in bacteria, *Cell Death Dis.* 6 (2015) e1609.
- [58] A. Tholudur, W.F. Ramirez, J.D. McMillan, Mathematical modeling and optimization of cellulase protein production using *Trichoderma reesei* RL-P37, *Biotechnol. Bioeng.* 66 (1999) 1–16.
- [59] K.L. Kadam, E.C. Rydholm, J.D. McMillan, Development and validation of a kinetic model for enzymatic saccharification of lignocellulosic biomass, *Biotechnol. Prog.* 20 (2004) 698–705.
- [60] Y. Zheng, Z. Pan, R. Zhang, B.M. Jenkins, Kinetic modeling for enzymatic hydrolysis of pretreated creeping wild ryegrass, 2009 Reno, Nevada, June 21–June 24, 2009, American Society of Agricultural and Biological Engineers, 2009, p. 1.
- [61] Y.J. Tang, R. Chakraborty, H.G. Martín, J. Chu, T.C. Hazen, J.D. Keasling, Flux analysis of central metabolic pathways in *Geobacter metallireducens* during reduction of soluble Fe (III)-nitrilotriacetic acid, *Appl. Environ. Microbiol.* 73 (2007) 3859–3864.
- [62] A.L. Meadows, R. Karnik, H. Lam, S. Forestell, B. Snedecor, Application of dynamic flux balance analysis to an industrial *Escherichia coli* fermentation, *Metab. Eng.* 12 (2010) 150–160.
- [63] M.A. Henson, P. Phalak, Microbiota dysbiosis in inflammatory bowel diseases: in silico investigation of the oxygen hypothesis, *BMC Syst. Biol.* 11 (2017) 145.
- [64] J.A. Gomez, K. Höffner, P. Barton, DFBAlab: a fast and reliable MATLAB code for dynamic flux balance analysis, *BMC Bioinformatics* 15 (2014) 409.